Thermal equilibrium noise with 1/f spectrum from frequency independent dielectric losses in barrium strontium titanate

Thermal equilibrium noise with 1/*f* spectrum from frequency independent dielectric losses in barium strontium titanate

L. K. J. Vandamme,[1,a] A. Khalfallaoui,[2] G. Leroy,[2] and G. Vélu[2]
[1]*Department of Electrical Engineering (PT 9.13), Eindhoven University of Technology, 5600MB Eindhoven, Netherlands*
[2]*Laboratoire d'Etude des Matériaux et des Composants pour L'Electronique, E.A. 2601, Université du Littoral Côte d'Opale, B.P. 717, 62 228 Calais, France*

(Received 23 October 2009; accepted 23 January 2010; published online 10 March 2010)

We investigated the dielectric losses of doped and undoped $BaSrTiO_3$ (BST) from thermal noise measurements. The results are compared to impedance measurements. The value for the frequency independent loss angle is about $tg\ \delta = 2 \times 10^{-2}$ in the range $100 < f(\mathrm{Hz}) < 10^5$. The thermal voltage noise of the BST capacitor with losses has a $1/f$ spectrum in agreement with $4kT\ \Re(Z)$ and a frequency independent $tg\ \delta$. The detection limits due to the low noise voltage amplifier are investigated and experimentally verified. The frequency range f_{high}, f_{low}, where the "$1/f$ thermal noise" is above the background noise is characterized by the ratio $f_{\mathrm{high}}/f_{\mathrm{low}} = tg^2\delta(R_{\mathrm{in}}/R_{\mathrm{eqw}})$, with R_{in} the input resistance of the low noise voltage amplifier and R_{eqw} the frequency independent part of its equivalent noise resistance at high frequencies. © *2010 American Institute of Physics*. [doi:10.1063/1.3327446]

I. INTRODUCTION

Barium strontium titanate (BST) is a promising dielectric for rf applications due to its high values of $\varepsilon_r (200 < \varepsilon_r < 600)$ and the fact that the value decreases by applying a positive or negative bias voltage, i.e., the tunability.[1,2] We have investigated the loss angle $tg\ \delta$ for doped and undoped BST from thermal noise in the frequency range $10 < f(\mathrm{Hz}) < 10^5$. The result without ac excitation is compared to impedance measurements.

The aim of this work is (i) to establish the detection limit for the noise measurements on capacitors with losses and (ii) to compare results from doped and undoped BST by thermal equilibrium and ac excitation measurements. The fluctuation dissipation theorem for these materials is applied.

Thermal equilibrium noise at low temperature ($T < 4$ K) with a $1/f$ spectrum was observed in the magnetic susceptibility of different materials.[3,4] Their results were in agreement with the fluctuation dissipation theorem as usual.

The loss tangent in dielectrics is often frequency independent over 8 decades in frequency.[5] The thermal $1/f$ noise in dielectrics with losses was discussed in Ref. 6 and thermal current noise proportional to f was experimentally verified in silicon p-n junctions in Ref. 7. For nanoparticle WO_3 films with a high value of the loss angle ($tg\ \delta = 1$), the detection of thermal current and voltage noise was easy and the analysis turned out to be in agreement with the fluctuation dissipation theorem. The noise of biased WO_3 and BST dielectrics was used as a diagnostic tool for dielectric quality assessment.[8,9] The losses in liquid crystals with $tg\ \delta > 0.1$ were also successfully investigated from noise measurements.[10]

However, detection problems arise when the loss angle of the material under test is smaller than 0.1. Our BST dielectrics have relatively low loss angles of about 10^{-2}, which makes a discussion of the detection limit unavoidable in Sec. II. In order to check detection problems, our noise measurements on BST capacitors with capacitance C are compared to the background noise of a variable air capacitor with negligible small $tg\ \delta$ with $C_{\mathrm{air}} = C$.

II. EXPECTED THERMAL NOISE FROM A CAPACITOR WITH LOSSES

A. Equivalent circuit of capacitor with losses and its thermal voltage noise

The equivalent circuit of a capacitor with a dielectric without free electrons is represented as shown in Fig. 1. For not too high frequencies, the circuit in Fig. 1(a) describes well the capacitor with losses. As a good approximation holds for frequencies below 10^5 Hz that C is frequency independent and R describing the losses is frequency dependent. The admittance and a more general presentation of the dielectric follow from Fig. 1(a)

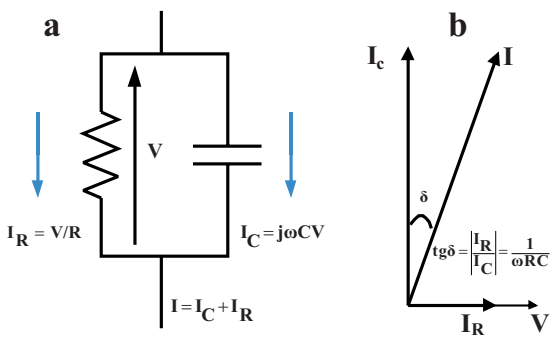

FIG. 1. (Color online) (a) Equivalent circuit of a capacitor with losses. (b) The definition of δ and $tg\ \delta$.

[a]Electronic mail: l.k.j.vandamme@tue.nl.

$$Y = j\omega C + \frac{1}{R} \equiv j\omega C^* = \frac{j\omega\varepsilon_0 A}{L}(\varepsilon' - j\varepsilon''),$$

with C^* the complex capacitance, $1/R = \omega\ \varepsilon_0\ \varepsilon'' A/L$, and $C = \varepsilon_0\ \varepsilon' A/L$.

Figure 1(b) shows the definition of the loss angle δ and $tg\ \delta$, which is the ratio between the current component in phase with the applied voltage V $|I_R|$ and the current component 90° out of phase $|I_C|$. The total current I makes an angle δ with I_C and $tg\ \delta$ is

$$tg\ \delta = \frac{1}{RC\omega} = \frac{\varepsilon''}{\varepsilon'}. \tag{1}$$

The $tg\ \delta$ is often frequency independent.[5] It is denoted as the ratio of the imaginary and real part of the complex capacitance C^*. The $tg\ \delta$ frequency independent means $R \propto 1/\omega$ if C is frequency independent or ε'' and ε' are frequency independent. If ε'' and ε' are proportional to $f^{-\Delta}$, then $tg\ \delta$ is still frequency independent.

The impedance Z, the real part of Z, $\Re(Z)$, and the real part of Y, $\Re(Y)$, are given by

$$Z = \frac{R}{1 + j\omega RC} \Rightarrow \Re(Z) = \frac{R}{1 + (\omega RC)^2} = \frac{tg\ \delta}{\omega C(1 + tg^2\delta)} \quad \text{for} \quad tg\ \delta \ll 1 \Rightarrow Re(Z) \approx \frac{tg\ \delta}{\omega C}, \tag{2}$$

$$Y = 1/R + j\omega C \Rightarrow Re(Y) = 1/R = \omega C\ \ tg\ \ \delta. \tag{3}$$

The expected thermal voltage noise in agreement with the fluctuation dissipation theorem for a capacitor with losses $S_{V_{\text{therm}}} = 4kT\ \Re(Z)$ is

$$S_{V_{\text{therm}}} = 4kT\frac{tg\ \delta}{\omega C(1 + tg^2\delta)} \propto \frac{1}{f}$$

for C and $tg\ \delta$ frequency independent

$$S_{V_{\text{therm}}} \cong 4kT\frac{tg\ \delta}{\omega C} \quad \text{or} \quad \frac{S_{V_{\text{therm}}}}{4kT} \cong R\ \ tg^2\delta \quad \text{for} \tag{4}$$

$$tg\ \delta \ll 1.$$

Hence, thermal $1/f$ voltage noise holds for C and $tg\ \delta$ frequency independent. If ε' and ε'' are weakly dependent on frequency and proportional to $f^{-\Delta}$ with often $\Delta < 0.2$, then still, $tg\ \delta$ is frequency independent but the thermal noise $S_{V_{\text{therm}}}$ is $1/f$ like noise proportional to $1/f^{(1-\Delta)}$.

The thermal current noise $S_{I_{\text{therm}}} = 4kT\ \Re(Y)$ is

$$S_{I_{\text{therm}}} = 4kT\ \Re(Y) = \frac{4kT}{R} = 4kT\ \ \omega C\ \ tg\ \ \delta \propto f \tag{5}$$

for C and $tg\ \delta$ frequency independent

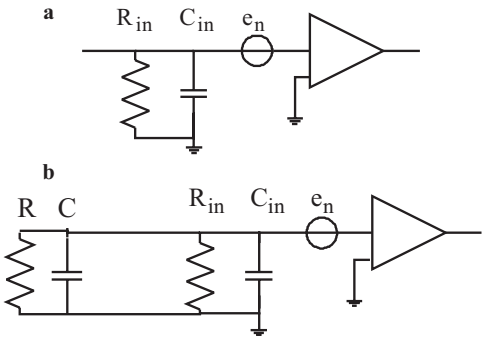

FIG. 2. (a) Equivalent circuit for a low noise amplifier. (b) Equivalent circuit of low noise amplifier with capacitor C and losses R.

$$\frac{S_{V_{\text{therm}}} S_{I_{\text{therm}}}}{(4kT)^2} = \frac{tg^2\delta}{1 + tg^2\delta} \cong tg^2\delta \quad \text{for} \quad tg\ \delta \ll 1. \tag{6}$$

Hence, the $tg\ \delta$ can be calculated from the thermal noise as shown in Eqs. (4)–(6). The ratio $S_{V_{\text{therm}}}/S_{I_{\text{therm}}}$ gives the squared value of the impedance

$$\frac{S_{V_{\text{therm}}}}{S_{I_{\text{therm}}}} = \frac{\Re(Z)}{\Re(Y)} = Z^2 = \frac{R^2}{1 + (\omega RC)^2} = \frac{1}{(\omega C)^2} \cdot \frac{1}{1 + tg^2\delta} \approx \frac{1}{(\omega C)^2} \quad \text{for} \quad tg\ \delta \ll 1. \tag{7}$$

B. Detection limits as a frequency range f_{low} and f_{high} for voltage noise

The detection below the lowest frequency f_{low} is limited by the thermal noise of the input resistance of the low noise voltage amplifier, and the detection above the highest frequency f_{high} is limited by the background noise of the amplifier with an ac short-circuited input. This is explained by using the equivalent circuit of a low noise voltage amplifier with input impedance Z_{in}, which is the parallel connection of input resistance R_{in} and input capacitance C_{in} as shown in Fig. 2(a). It will be used to calculate the frequency range, where thermal voltage noise detection of the capacitor with losses $C//R$ as shown in Fig. 1(a) is possible. Figure 2(a) shows a noise voltage source e_n at the input, an ideal (infinite input impedance) noise-free amplifier with the same gain and bandwidth $f_{h\ \text{amp}} - f_{l\ \text{amp}}$ as the real amplifier.

For low noise voltage amplifiers with an open input holds $S_{V_{\text{open}}} = 4kT\ \Re(Z_{\text{in}}) + \langle e_n^2 \rangle$. For good low noise amplifiers with open input holds at $f \approx f_{l\ \text{amp}}$, $S_{V_{\text{open}}} = 4kT\ R_{\text{in}}$. The noise of an amplifier with short-circuited input is often white above a characteristic frequency $f_0 (f_0 \leq 300\ \text{Hz})$ and proportional to $1/f$ below f_0. Therefore, the voltage noise with short-circuited input $\langle e_n^2 \rangle = S_{V_{\text{short}}}$ is often characterized by R_{eq}, the equivalent noise resistance of an amplifier at room temperature as

$$S_{V_{sh}} = 4kTR_{eq} = 4kTR_{eqw}\left(1+\frac{f_0}{f}\right) \Rightarrow \frac{S_{V_{short}}}{4kT} = R_{eqw}\left(1+\frac{f_0}{f}\right), \quad (8)$$

with R_{eqw} representing the white part of the spectrum $S_{V_{short}}$ and hence, R_{eqw} is the value of R_{eq} at $f \gg f_0$. For high quality low noise amplifiers holds (i) $R_{in} \gg R_{eqw}(1+f_0/f)$; (ii) for $S_{V_{open}}$

$$S_{V_{open}} \cong \frac{4kTR_{in}}{1+(\omega R_{in}C_{in})^2} + 4kTR_{eqw} \Rightarrow \frac{S_{V_{open}}}{4kT} = \frac{R_{in}}{1+(\omega R_{in}C_{in})^2} + R_{eqw}. \quad (9)$$

The voltage noise of the amplifier with open input $S_{V_{open}}$ in Eq. (9) is approximated in three regions: low, $f<f_1$; medium, $f_1<f<f_2$; and high frequency $f>f_2$ as, respectively,

$$S_{V_{open}} = 4kTR_{in} \quad \text{for} \quad f_{l\ amp} < f < f_1 = \frac{1}{2\pi R_{in}C_{in}},$$

$$S_{V_{open}} = \frac{4kT}{R_{in}(\omega C_{in})^2} \quad \text{for} \quad f_1 < f < f_2 = f_1\sqrt{\frac{R_{in}}{R_{eqw}}},$$

$$S_{V_{open}} = 4kTR_{eqw} \quad \text{for} \quad f_2 < f < f_{h\ amp}. \quad (10)$$

Hence, for open input [Eq. (9)], two corner frequencies can be distinguished

$$f_1 = 1/(2\pi R_{in}\ C_{in}) \quad \text{and} \quad f_2 = 1/[2\pi(R_{in}\ R_{eqw})^{1/2}C_{in}] = f_1(R_{in}/R_{eqw})^{1/2}.$$

The background noise for voltage noise measurements of capacitors with losses is calculated from Fig. 2(b) by replacing C by an air capacitor with $tg\ \delta=0$ and a value $C_{air}=C$ and $R\to\infty$. For calibration purposes and the calculation of the detection limits, a spectrum is calculated and measured from an air capacitor $C_{air}=C$ with negligible losses. The spectrum $S_{V\ C_{air}}$ with C_{air} and $tg\ \delta \approx 0$ is the background noise for noise based $tg\ \delta$ measurements. The relation for $S_{V\ C_{air}}$ is given by Eq. (9), where C_{air} is added to C_{in}. The corner frequencies are now $f_{1(C_{air})}$ and $f_{2(C_{air})}$ and are a factor $(1+C_{air}/C_{in})$ lower than f_1 and f_2 given in Eq. (10). The background noise can be approximated in analogy with Eq. (10) by three frequency regions

$$S_{V\ C_{air}} = 4kTR_{in} \quad \text{for} \quad f_{l\ amp} < f < f_{1(C_{air})} = \frac{f_1}{1+C_{air}/C_{in}}, \quad (11)$$

$$S_{V\ C_{air}} = \frac{4kT}{R_{in}[\omega(C_{in}+C_{air})]^2} \quad \text{for} \quad f_{1(C_{air})} < f < f_{2(C_{air})} = \frac{f_2}{1+C_{air}/C_{in}}, \quad (12)$$

$$S_{V\ C_{air}} = 4kTR_{eqw} \quad \text{for} \quad f_{2(C_{air})} = \frac{f_2}{1+C_{air}/C_{in}} < f < f_{h\ amp}. \quad (13)$$

The noise $S_{V_{C//R}}$ of a capacitor C with losses is evaluated from the total impedance Z_t at the input in Fig. 2(b). The real part of the total impedance $\Re(Z_t)$ is given by Eq. (2), where C is replaced by $(C+C_{in})$ and R is replaced by $(R//R_{in})$ that is given by

$$(R//R_{in}) = \frac{R_{in}R}{R_{in}+R} = \frac{R_{in}}{1+\omega R_{in}C\ tg\ \delta}. \quad (14)$$

From Eq. (14) we define the corner frequency f_{low}

$$f_{low} = \frac{1}{2\pi R_{in}C\ tg\ \delta}. \quad (15)$$

Below f_{low}, the detection of losses $(tg\ \delta)$ from thermal noise measurements is impossible. The parallel connection of losses and input resistance $(R//R_{in})$ is approximately equal to R_{in}. The input impedance of the amplifier is the limiting factor.

The voltage noise $S_{V_{C//R}}$ is given by

$$S_{V_{C//R}} = \frac{4kT(R//R_{in})}{1+[\omega(R//R_{in})(C+C_{in})]^2} + 4kTR_{eqw} \quad (16)$$

and Eq. (16) is approximated for medium frequencies $f_{low}<f<f_{high}$ as

$$\frac{S_{V_{C//R}}}{4kT} \cong \frac{R}{1+[\omega R(C+C_{in})]^2} = \left(\frac{tg\ \delta}{C\omega}\right)\frac{1}{tg^2\delta+(1+C_{in}/C)^2} \quad (17)$$

for $tg\ \delta \ll 1$, and $C_{in}/C \ll 1$ holds $(S_{V_{C//R}}/4kT) \cong (tg\ \delta/C\omega)$.

The observed noise above the corner frequency f_{high} will be white due to the term $4kTR_{eqw}$ in Eq. (16) and the detection of the losses by noise is impossible. This occurs at $f>f_{high}$ defined as

$$\frac{S_{V_{C//R}}}{4kT} = \frac{tg\ \delta}{\omega C} = R_{eqw} \Rightarrow f_{high} = \frac{tg\ \delta}{2\pi R_{eqw}C}. \quad (18)$$

Summarizing the measured thermal voltage noise $S_{V_{C//R}}$ with a $1/f$ spectrum equals the expected value given in Eq. (4) only for the medium frequencies

$$S_{V_{C//R}} = \frac{4kT\ tg\ \delta}{\omega C} \quad \text{for} \quad f_{low} = \frac{1}{2\pi R_{in}C\ tg\ \delta} < f < f_{high} = \frac{tg\ \delta}{2\pi R_{eqw}C}. \quad (19)$$

For a frequency independent loss angle and C, the spectrum is proportional to $1/f$.

For the highest frequencies holds,

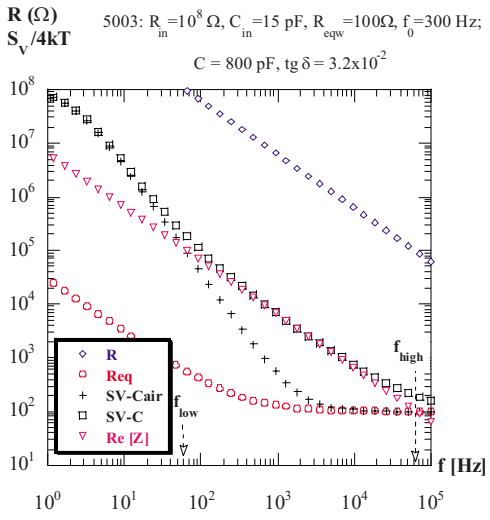

FIG. 3. (Color online) R vs f for a capacitor $C=800$ pF and frequency independent $tg\ \delta=3.2\times10^{-2}$. The equivalent noise resistance of the amplifier R_{eq} vs f with $f_0=300$ Hz and $R_{eqw}=100\ \Omega$ and the expected thermal noise proportional to $\Re(\mathbf{Z})$ vs f. The calculated background noise with $C_{air}=C$ and $R_{in}=10^8$ is labeled by crosses and show the typical $1/f^2$ proportionality between the levels R_{in} and R_{eqw}. The calculated noise of the capacitor with losses is denoted by squares and takes into account the effects of the nonideal low noise amplifier ($f_0=300$ Hz and $R_{eqw}=100\ \Omega$; $R_{in}=10^8\ \Omega$ and $C_{in}=15$ pF). The detection frequency range f_{high} and f_{low} is indicated by arrows.

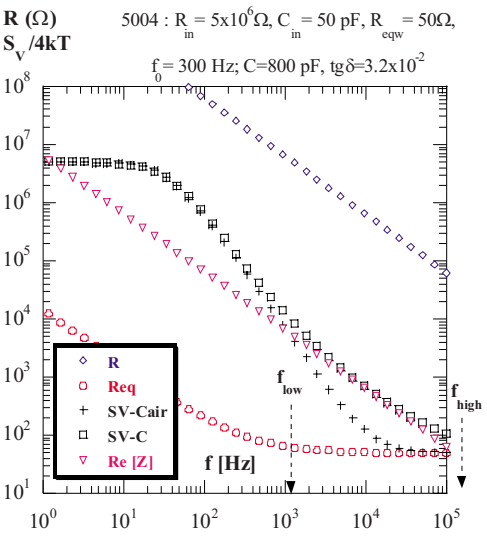

FIG. 4. (Color online) The same as in Fig. 3 but now for an amplifier characterized by $f_0=300$ Hz and $R_{eqw}=50\ \Omega$; $R_{in}=5\times10^6\ \Omega$ and $C_{in}=50$ pF.

$$S_{V_{C//R}}=4kTR_{eqw} \quad \text{for} \quad f>f_{high}=\frac{tg\ \delta}{2\pi\ R_{eqw}C}. \tag{20}$$

The $tg\ \delta$ can be extracted from thermal voltage noise measurement in the frequency range

$$f_{low}=\frac{1}{2\pi R_{in}C\ tg\ \delta}<f<f_{high}=\frac{tg\ \delta}{2\pi R_{eqw}C}. \tag{21}$$

From Eq. (21) follows the ratio of the detection limits f_{high}/f_{low} as

$$\frac{f_{high}}{f_{low}}=tg^2\delta\frac{R_{in}}{R_{eqw}}. \tag{22}$$

The use of an amplifier with a high ratio R_{in}/R_{eqw} is a necessary condition to detect $tg\ \delta$ from thermal $1/f$ voltage noise over several decades in f. Typical values for low noise voltage amplifiers are $R_{in}=10^8\ \Omega$, $R_{eqw}=70\ \Omega$, and $C_{in}=15$ pF (Brookdeal 5003). To demonstrate the importance of a high ratio R_{in}/R_{eqw}, we calculated spectra expressed as $S_V/4kT$ (equivalent noise resistance) and the detection limits. The results for two amplifiers are shown in Figs. 3 and 4 with the values for R_{in}, C_{in}, R_{eqw}, and f_0 as indicated on top of the diagram. The detection limits f_{low} and f_{high} are indicated by arrows. The circles show R_{eq} versus f. The diamonds show R versus f. The triangles show the expected thermal noise with a $1/f$ spectrum Eq. (4) from $C=800$ pF, with a frequency independent $tg\ \delta=3.2\times10^{-2}$. The crosses show the calculated noise with a loss-free air capacitor and nonideal amplifier. The calculated and experimentally observed background noise shows the typical $1/f^2$ proportionality between a high and low plateau level given by R_{in} and R_{eqw}, respectively. The squares show the calculated noise of a capacitor with losses.

The detection of thermal current noise from capacitors with loss angles $tg\ \delta<2\times10^{-2}$ is below the detection level of most commercially available low noise current amplifiers with an open input current noise of about $2\times10^{-28}\ A^2/Hz$ and will, therefore, not be discussed here.

III. EXPERIMENTAL RESULTS

A. Sample preparation

The sol-gel technique was used to deposit undoped and Mn-doped and K-doped BST films. The precursors used in the preparation of the solution are barium acetate, strontium acetate, manganese acetate, and kalium acetate. Acetic acid and isopropanol were used as the solvent. Barium acetate and strontium acetate were dissolved in hot acetic acid. Barium and strontium are in the concentration of 0.5 mol of the site A in the perovskite structure. The dopant precursor was in a concentration between 2.5 and 10 mol % of the substituted site. After getting a clear solution, titanium isopropoxide was added to obtain the final precursor solution. After total dissolution ethylene glycol was added to improve the stability.

The precursor solution was spin coated on platinum coated silicon (100) substrates by a spinner at 3000 rpm for 30 s. The samples were heated for 30 s on a hot plate at 300 °C. Afterwards, in order to crystallize the films in the perovskite phase, thermal annealing at 750 °C was used in a tubular furnace. Finally, gold was evaporated through a metallic shadow mask to realize the upper circular electrodes with diameters ranging from 150 μm to 2 mm. The thickness of the undoped layers was 600 and 430 nm for the Mn-doped and 400 nm for the K-doped BST. The Pt/Ti layer acts as the bottom electrode. More details on the BST films can found in Ref. 11.

The electrical properties were determined at room temperature in the frequency range 100 Hz–1 MHz as function of dc bias with the HP 4284A impedance analyzer.

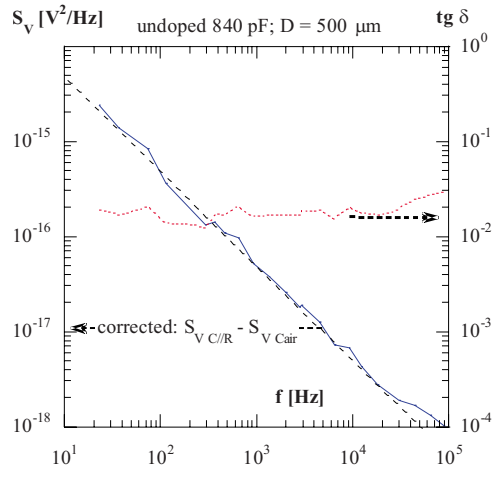

FIG. 5. (Color online) The full line is $S_{V_{C//R}}-S_{V\ C_{air}}$ with the $1/f$ proportionality typical for a frequency independent loss angle. The dashed line is a guide for the eye with $1/f$ slope. The dotted line represents the $tg\ \delta$ vs f with the right hand scale. The calculated value for $tg\ \delta$ from thermal $1/f$ noise measurement and Eq. (19) is about 2×10^{-2} and is reliable in the frequency range $f_{low}=95$ Hz and $f_{high}=5.4\times10^{4}$ Hz.

B. Thermal noise voltage

The spectra are measured with a Brookdeal 5003 low noise voltage amplifier with $R_{in}=10^{8}\ \Omega$, $C_{in}=15$ pF, and $R_{eqw}=70\ \Omega$. The detection is limited in the frequency range f_{low} and f_{high} and is calculated with Eqs. (15) and (18).

The results of an undoped BST sample with a diameter of 500 μm are shown in Fig. 5. The spectrum $S_{V_{C//R}}$ corrected for $S_{V\ C_{air}}$ is used to calculate $tg\ \delta$. In the frequency range between $f_{low}=90$ Hz and $f_{high}=4\times10^{4}$ Hz, reliable values for $tg\ \delta$ are obtained. The loss angle $tg\ \delta\approx2\times10^{-2}$ and is constant over 3 decades in frequency as can be seen from the dotted line versus the right hand scale.

The results for K-doped BST with a diameter of 500 μm are in Fig. 6. K-doped BST shows a slightly higher ε' than the undoped BST. The open squares show the background noise with air capacitor $S_{V\ C_{air}}$. The experimentally observed background noise shows the typical $1/f^{2}$ proportionality between a high and low plateau level given by R_{in} and R_{eqw}, respectively. The full squares show $S_{V_{C//R}}$. The full line shows $S_{V_{C//R}}-S_{V\ C_{air}}$ with the typical $1/f$ proportionality. The calculated $tg\ \delta$ versus the right hand scale results in reliable values between the detection limits $f_{low}=50$ Hz and $f_{high}=4\times10^{4}$ Hz.

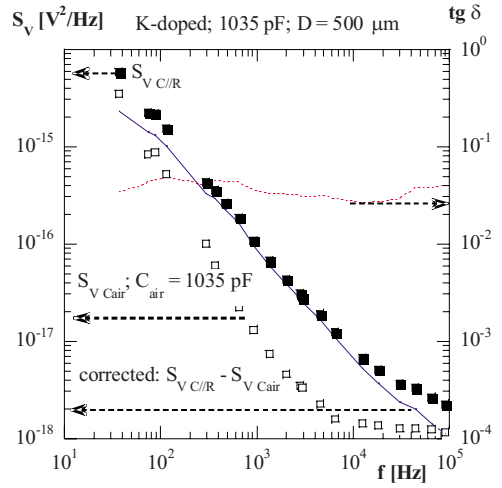

FIG. 6. (Color online) The results from a K-doped BST sample with a diameter $D=500$ μm and $C=1035$ pF. The dotted line represents $tg\ \delta$ calculated from the thermal $1/f$ noise given by the full line ($S_{V_{C//R}}-S_{V\ C_{air}}$). Reliable results for $tg\ \delta$ are between $f_{low}=40$ Hz and $f_{high}=7\times10^{4}$ Hz. The $S_{V_{C//R}}$ is denoted by full squares and the background noise $S_{V\ C_{air}}$ is shown by open squares.

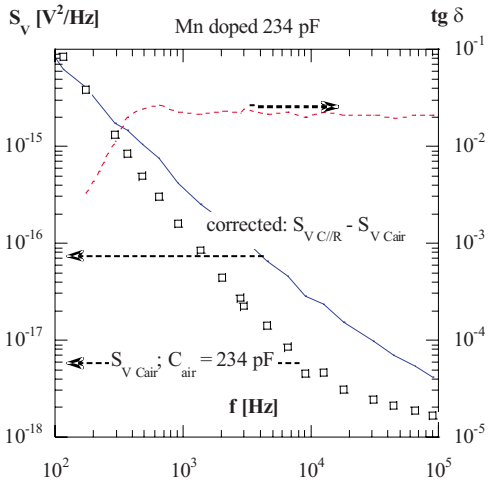

FIG. 7. (Color online) The results from a Mn-doped sample of 234 pF with a diameter of 250 μm. The full line is $S_{V_{C//R}}-S_{V\ C_{air}}$ with the $1/f$ proportionality typical for a frequency independent loss angle. The open squares show the background noise $S_{V\ C_{air}}$. The dotted line represents $tg\ \delta$. The reliable values for $tg\ \delta=2\times10^{-2}$ are between $f_{low}=400$ Hz and $f_{high}=10^{5}$ Hz. The smaller C (smaller diameter) compared to the C of samples in Figs. 5 and 6 results in higher values for f_{low} and f_{high} [see Eqs. (15) and (18)].

Figure 7 shows the results of a 234 pF Mn-doped BST sample with a diameter of 250 μm. The open squares show the background noise with an air capacitor, $S_{V\ C_{air}}$. The full line shows $S_{V_{C//R}}-S_{V\ C_{air}}$. The dotted line represents $tg\ \delta$ versus the right hand scale.

Figure 8 shows the comparison between the results from thermal voltage noise (open symbols) and impedance measurements (full symbols). Experimental artifacts are visible below 10 kHz due to the impedance measurement system. Hence, an increase in $tg\ \delta$ with a decrease in f is erroneously suggested.

The largest frequency range in order to observe reliable $tg\ \delta$ values from thermal noise with an amplifier character-

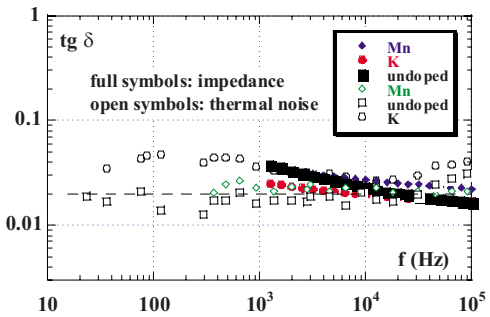

FIG. 8. (Color online) Comparison between $tg\ \delta$ from impedance (full symbols) and noise measurements (open symbols).

ized by $R_{in}=10^8\ \Omega$, $C_{in}=15$ pF, $f_0=300$ Hz, and $R_{eqw}=70\ \Omega$ is for samples with a capacitance of about 1000 pF.

IV. DISCUSSION AND CONCLUSION

To get reliable values for the loss angle from thermal noise measurements, a correction for the background noise obtained with an air capacitor without losses is a necessary condition especially at frequencies around f_{low} and f_{high}. Ignoring the correction at low frequencies leads to an erroneous increase in $tg\ \delta$ with decreasing frequency, and at high frequencies an erroneous increase in $tg\ \delta$ with increasing frequency is the result; overcorrection leads to opposite results.

The observed voltage noise at high frequencies ($f > f_{high}$) of a capacitor with losses is larger than $4kT\ \Re(Z)$ with Z the impedance of the capacitor under investigation. At high frequencies the low noise voltage amplifier has an ac short-circuited input and the voltage noise of the amplifier must be subtracted.

The loss angle ($tg\ \delta$) can be calculated from the thermal voltage noise in a limited frequency range $1/(2\pi R_{in}C\ tg\ \delta) < f < tg\ \delta/(2\pi\ R_{eqw}C)$.

From the thermal noise measurement we observe reliable values for $tg\ \delta$ for $10^3 < f(\mathrm{Hz}) < 10^5$. The loss angle is frequency independent with an average value of about 2×10^{-2} for all BST samples. The K-doped have slightly higher $tg\ \delta$ values and the undoped slightly lower. Dielectrics with high ε' values that are strongly voltage dependent are better measured from the thermal noise in equilibrium especially at frequencies below 10^4 Hz.

In general, the possible link between the $1/f$ thermal voltage noise and the $1/f$ noise due to resistance fluctuations should be distinguished carefully.[6] Kleinpenning[12,13] made an exception where the $1/f$ noise in tunnel junctions was related to a constant loss tangent of the insulator in between the two metal electrodes. Then the transparency factor of the barrier is modulated by the thermal $1/f$ noise (if $tg\ \delta$ and C are frequency independent) with $1/f$ noise in the conduction as a result.

[1] G. Vélu, L. Burgnies, G. Houzet, K. Blary, D. Lippens, and J.-C. Carru, Integr. Ferroelectr. **93**, 110 (2007).
[2] L. Burgnies, G. Vélu, K. Blary, J.-C. Carru, and D. Lippens, Electron. Lett. **43**, 1151 (2007).
[3] B. Barbara, A. Ratman, A. Cavalleri, M. Cerdonio, and S. Vitale, J. Appl. Phys. **75**, 5634 (1994).
[4] G. Durin, P. Falferi, M. Cerdonio, G. A. Prodi, and S. Vitale, J. Appl. Phys. **73**, 5363 (1993).
[5] A. K. Jonscher, *Dielectric Relaxation in Solids* (Chelsea Dielectrics, London, 1983).
[6] G. Galeczki, J. Hajdu, and L. B. Kiss, Solid State Commun. **72**, 1131 (1989).
[7] M. Akiba, Appl. Phys. Lett. **71**, 3236 (1997).
[8] A. Hoel, L. K. J. Vandamme, L. B. Kish, and E. Olsson, J. Appl. Phys. **91**, 5221 (2002).
[9] G. Leroy, G. Vélu, J. Gest, L. K. J. Vandamme, and J.-C. Carru, Proceedings of the OHD Conference, 2003, Calais, France (unpublished), B4–2.
[10] G. Leroy, J. Gest, and P. Tabourier, Fluct. Noise Lett. **1**, L125 (2001).
[11] G. Vélu, J.-C. Carru, E. Cattan, D. Remiens, X. Melique, and D. Lippens, Ferroelectrics **288**, 59 (2003).
[12] T. G. M. Kleinpenning, Solid-State Electron. **21**, 927 (1978).
[13] T. G. M. Kleinpenning, Solid-State Electron. **25**, 78 (1982).